

https://doi.org/10.1070/QEL17593

Effect of elastic anisotropy on thermally induced distortions of a laser beam in single cubic syngony crystals with radial cooling. Part III

A.G. Vyatkin

Abstract. **We report a study of thermally induced depolarisation of a laser beam in single cubic syngony crystals of 23 and m3 symmetry groups with an anisotropic elastic stiffness tensor. For active elements in the form of a long rod and a thin disk with radial cooling under uniform volume pumping, we investigate the effect of anisotropy of elastic properties on the dependence of the degree of depolarisation in the crystal on the orientation of the crystallographic axes, as well as on the position of the critical orientation in the crystallographic coordinate system.**

Keywords: *high average power lasers, photoelastic effect, thermally induced depolarisation, anisotropy of cubic crystals.*

1. Introduction

Thermal effects are an important factor limiting the power and quality of the output radiation of solid-state lasers [1, 2]. Thermally induced depolarisation of radiation in initially optically isotropic media – cubic single crystals, glasses, and ceramics – has been studied theoretically and experimentally since the 1960s. Except for few works, in cubic crystals, as a rule, only the anisotropy of the photoelastic effect is taken into account, whereas the elastic properties of materials are considered to be isotropic (see [3] and references therein). However, already at the beginning of research it was known that this was only an approximation, and a solution to the elasticity problem for a parabolic temperature profile was found [4].

We study thermally induced beam distortions in single cubic syngony crystals of all symmetry groups taking into account the anisotropy of their elastic properties, as well as at an arbitrary orientation of the crystallographic axes. In the first part of our work (paper [3]), we obtained expressions for the phase and polarisation distortions of the beam in active elements in the form of a long rod and a thin disk. We found eighenpolarisations, as well as the arithmetic mean and the difference between the incursions of their phases; considered the specific orientations of crystals; and determined the effective values of the thermo-optical constants P and Q. In the second part of our work (paper [5]), we studied thermally induced depolarisation in single crystals of symmetry groups 432, $\bar{4}3m$, and m3m. This paper – the third part of our work – is devoted to the analysis of thermally induced depolarisation of radiation in elastically anisotropic single crystals of symmetry groups 23 and m3 in comparison with the elastically isotropic case and to finding optimal orientations of crystallographic axes under weak and strong birefringence, which makes it possible to minimise the degree of depolarisation. In Section 2 we introduce the notations necessary for the statement of the problem. In Section 3 we determine the specific orientations in m3 crystals, and in Section 4 we investigate the degree of depolarisation in single crystals for which critical orientation is absent. In Section 5 we examine the critical orientation in crystals with a negative value of the first parameter of the photoelastic anisotropy.

A.G. Vyatkin Institute of Applied Physics, Russian Academy of Sciences, ul. Ulyanova 46, 603950 Nizhny Novgorod, Russia; e-mail: vyatkin@appl.sci-nnov.ru

Received 1 October 2020; revision received 30 April 2021
Kvantovaya Elektronika **51** (7) 574–581 (2021)
Translated by I.A. Ulitkin

2. Statement of the problem and some notations

In the framework of this work, we restrict ourselves to media that do not rotate the polarisation plane. We will consider an active element in the form of a cylinder, the z axis of which coincides with the propagation direction of probe radiation. This element can be cut from the bulk of a crystal in various directions and is uniquely specified by the position of its axis in the crystallographic coordinates. This can be done using the first two of the three Euler angles – azimuthal (α) and polar (b) (see Figs 1a, 1b, and 1d in [3]), while the third Euler angle (Φ) will be equal, with the opposite sign, to the angle of rotation of the active element around its axis relative to the laboratory coordinate system (see Figs 1c and 1d in [3]).

It is customary to say that a pair of Euler angles (α, β) defines the orientation of the crystal, also denoted by the Miller indices [MNP]. In this paper, major attention is paid to [$M0N$] and [MMN] orientations shown in Fig. 1. Following the generally accepted approach, we will not distinguish between orientations obtained from each other by

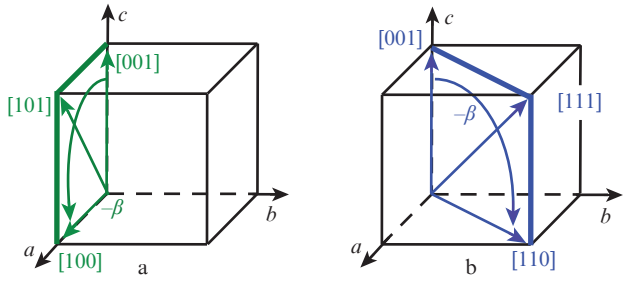

Figure 1. (a) Orientations [$M0N$] ($\alpha = 0$) in the crystallographic coordinate system (a, b, c) and (b) orientations [MMN] ($\alpha = \pi/4$).

cyclic permutation of indices ([*NPM*], [*PMN*]) and changing the signs of indices ([$MN\bar{P}$], [$\bar{M}N\bar{P}$], etc.) due to their equivalence [6].

Let us consider an active element in the form of a long rod or thin disk of radius R, heated uniformly throughout the bulk and cooled through the lateral surface. The temperature and elastic stress fields are given in [3] and do not depend on z, if we neglect the end effects in the rod.

The lateral cooling of a thin disk is not optimal, but it allows the degree of depolarisation to be calculated analytically. We believe that the regularities we have identified will be applicable in the case of end-face heat removal, despite the impossibility of a quantitative assessment of thermally induced beam distortions.

The local degree of depolarisation Γ is commonly referred to as the fraction of the radiation intensity that has passed during propagation through a birefringent optical system into the polarisation that is orthogonal to the initial one. A similar fraction of power is called the integral degree of depolarisation. In the plane wave approximation, it is easy to obtain that after a laser beam, initially linearly polarised in the perpendicular plane xy at an angle θ to the x axis, passes along the axis of one active element, the permittivity tensor of which is independent of z, the local degree of polarisation is expressed as

$$\Gamma(x,y) = \sin^2(\delta/2)\sin^2[2(\Psi-\theta)], \tag{1}$$

where $\Psi(x,y)$ is the angle of inclination of the polarisation vector of one of the eigenwaves in the active element, and $\delta(x,y)$ is the difference between the incursions of their phases. Averaging (1) over the cross section of the probe beam with the field intensity $\boldsymbol{E}_{\text{in}}(x,y)$, we obtain the integral degree of depolarisation

$$\gamma = \left(\iint_S |\boldsymbol{E}_{\text{in}}|^2 \mathrm{d}S\right)^{-1} \iint_S \Gamma |\boldsymbol{E}_{\text{in}}|^2 \mathrm{d}S \tag{2}$$

(for simplicity, we assume that there is no absorption and amplification of probe radiation in the medium). With strong birefringence, γ tends to a steady-state value

$$\gamma_\infty = \left(\iint_S |\boldsymbol{E}_{\text{in}}|^2 \mathrm{d}S\right)^{-1} \iint_S \tilde{\Gamma}_\infty |\boldsymbol{E}_{\text{in}}|^2 \mathrm{d}S, \tag{3}$$

where $\tilde{\Gamma}_\infty = \frac{1}{2}\sin^2[2(\Psi-\theta)]$ (see [7] and Fig. 2 from [5]).

In [3] we obtained expressions for δ and Ψ in crystals with anisotropic elastic properties. Without going into details here, we note that they differ in a thin disk and a long rod, as well as that δ is proportional to the dimensionless heat release power in an optical element and Ψ is independent of it. In the calculations, we use the dimensionless heat release power p, which was generalised to elastic anisotropic media in [3].

Cubic crystals can be divided into two types according to the form of their material tensors. In [5], crystals of the m3m, 432, and $\bar{4}3$m symmetry groups were considered, which we agreed to call m3m crystals [3]. Their material tensors of the 4th rank, the piezo-optical tensor $\boldsymbol{\pi}$ and the elastic compliance tensor $\boldsymbol{s}$, are determined by three independent nonzero coefficients, and their general form in two-index Nye notation is schematically presented in [8], as well as in Fig. 2a from [3]. In this paper, we will consider other cubic syngony crystals belonging to m3 and 23 symmetry groups, which we call m3 crystals. For them, the tensor $\boldsymbol{s}$ is the same, and the tensor $\boldsymbol{\pi}$ is determined by four independent coefficients (see Fig. 2b from [3]) [8].

The dependence of thermally induced beam distortions on the orientation of crystallographic axes in cubic crystals in the approximation of an isotropic elasticity problem is determined by the photoelastic anisotropy parameter ξ [7, 9], for which we use the piezo-optical ratio, taking into account the m3 symmetry properties. The photoelastic anisotropy parameter has the form [6]

$$\begin{aligned} &\xi_\pi = \pi_{66}/\pi_s, \\ &\pi_s = \pi_{11} - \frac{1}{2}(\pi_{12} + \pi_{21}). \end{aligned} \tag{4}$$

It was also shown there that in m3 crystals, along with the parameter ξ, it is necessary to determine the second parameter of photoelastic anisotropy

$$\xi_d = (\pi_{12} - \pi_{21})/\pi_s. \tag{5}$$

In m3m crystals

$$\begin{aligned} &\pi_s = \pi_{11} - \pi_{12}, \\ &\xi_d = 0. \end{aligned} \tag{6}$$

In [3], we obtained that, in media with anisotropic elastic properties, the dependence of thermally induced beam distortions on orientation is modulated by functions that are determined by a combination of Poisson's ratio $\nu_{[001]}$ for the [001] orientation [10] with the elastic anisotropy parameter

$$\xi_s = \frac{s_{66}}{2(s_{11} - s_{12})}. \tag{7}$$

For different orientations of the crystallographic axes, let us compare the degree of thermally induced depolarisation calculated for elastically anisotropic cubic single crystals in the form of a long rod and a thin disk with that calculated in the isotropic elasticity approximation. We will focus on choosing the optimal orientation. Since in the experiment the angle Φ of rotation of the crystal, in contrast to the other Euler angles, can be easily changed after the manufacturing of the active element, we will investigate the degree of depolarisation that is minimal in Φ, which we will call optimal. To simplify the calculations, we will assume that the probe beam has a flat-top transverse profile of the radiation intensity. Such beams are often generated in high-power multistage laser systems. Moreover, this assumption does not qualitatively affect the results. The beam radius is denoted by r_0.

Recently, crystals of yttrium, scandium and lutetium sesquioxides have been of interest (see papers [11–13] and references in [6]). However, the photoelastic properties of Y_2O_3 and Sc_2O_3 are known only partially [14], and there are no data on Lu_2O_3. Complete data are available only for rarely used crystals, and were often obtained quite a long time ago [8, 15]. Therefore, we also use in our calculations hypothetical media obtained by changing the properties of popular optical materials.

3. Specific orientations in elastically anisotropic m3 single crystals

In m3 crystals, the photoelastic effect has a reduced symmetry due to a lower symmetry of the crystal lattice than in m3m

crystals. Of the three simplest orientations, only the [111] orientation retains its symmetry: the [001] orientation has a lower symmetry, while the [011] orientation does not have any at all [8]. In work [6], we showed that the special properties that the photoelastic effect exhibits in m3m crystals with these orientations are observed in elastically isotropic m3 crystals with more general [*M*0*N*] orientations, which we called [[A]] and [[B]]. The position of these orientations in crystals is determined by the ratio

$$q_d = \xi_d/(\xi_\pi - 1). \quad (8)$$

In Section 5.2 of work [3], we showed that in an elastically anisotropic disk, as well as in the approximation of weak elastic anisotropy {see (50) in [3]} in a long rod, the [[A]] orientation is specific, and the [[B]] orientation is present only in a disk; in a rod, it takes a new position, which we have denoted by [[B$_\sim$]]. With a stronger elastic anisotropy in the rod, the specific orientations should change, but no analytical expressions were obtained for the corresponding Euler angles.

The specific orientations [[C]] and [[D]] in m3 crystals, in contrast to m3m crystals, do not belong to the [*MMN*] set.

At the same time, the elastic compliance tensor retains the same symmetry as in m3m crystals, and this symmetry is inherited by the dependences of the stress tensor components on the crystal orientation. Thus, thermally induced beam distortions in elastically anisotropic m3 crystals are determined by a combination of two material tensors with different symmetries.

On the other hand, it was noted in [6] that the optimal orientations of the crystallographic axes of elastically isotropic m3 crystals coincide with the specific orientations [[A]] and [[B]] only for probe beams of small radii, while for m3m crystals one of the simplest orientations is optimal for any beam profile [7]. It is obvious that taking into account the effects of elastic anisotropy in m3 crystals can lead to a shift in orientations that are optimal from the point of view of depolarisation relative to both elastically isotropic and specific orientations. Let us consider the problem of the position of optimal orientations in m3 crystals with different photoelastic properties.

4. Thermal depolarisation in m3 single crystals without critical orientation

It should be recalled that in m3 crystals the critical orientation is absent not only for $\xi_\pi > 0$, but also for $\xi_\pi < -3$, provided that $|\xi_d|$ exceeds the threshold value, greater than two. This value was determined in [6] and in (79) from [3] in the elastically isotropic approximation and in a thin disk. In the absence of the critical orientation, thermally induced depolarisation, as a rule, is minimised for one of the orientations of the [*M*0*N*] set [6]. As in m3m crystals, the behaviour of the degree of depolarisation in these orientations is qualitatively different, depending on the value of $|\xi_\pi|$.

4.1. Case of $|\xi_\pi| > 1$

Figure 2 shows the optimal degree of depolarisation γ in model m3 single crystals with the same elastic parameters $\nu_{[001]}$ and ξ_s as for CaF_2, the parameter ξ_π as for YAG, and three different ξ_d: small ($q_d \approx 0.045$), average ($q_d \approx 0.45$) and large ($q_d \approx 1.045$). The calculation was performed for relatively small ($p = 1, \gamma \ll \gamma_\infty$) and large ($p \gg 1, \gamma = \gamma_\infty$) dimensionless heat release powers, as well as for probe beams of large (0.8*R*) and small (0.4*R*) radii. As in m3m crystals, in the case of weak birefringence, the degree of depolarisation differs from the elastically isotropic one by an order of tens of percent. However, this difference quantitatively depends on the method for determining the isotropic elastic moduli (see Section 3 in [5]). The kinks in the curves at $p = 1$ are due to the fact that the optimal value of the angle Φ changes by 45°.

One can see from the figure that with weak birefringence, the optimal orientation is close to the analytical estimate [[A]], and for a thin probe beam, as we noted in [6], the estimate works better. With strong birefringence, in the case of a thin probe beam, the optimal orientation is close to the estimates [[B]] and [[B$_\sim$]] in the disk and in the rod, respectively, and in the case of a wide beam, to [[A]]. Note that [[B]] estimates the worst orientation with less accuracy, while in the rod [[B$_\sim$]] can work worse than [[B]] (Figs 2h and 2k).

Note that the degree of depolarisation in the disk under strong birefringence coincides with the result of the elastic isotropic calculation (this property was already discussed in Section 5.1 of [3] and in Section 3 of [5]). In other cases for both considered crystal geometries allowance for the anisotropy of elasticity leads to a slight shift in the optimal orientation of the crystal relative to the elastic isotropic one. We can also note the good accuracy of the simplified Sirotin solution for the rod, which deteriorates slightly with increasing $|\xi_d|$. The degree of depolarisation for the [011] orientation remains independent of ξ_d (see theorem 6 in [6]) in elastic anisotropic media as well. The minimum of the degree of depolarisation under weak birefringence is sharp (Figs 2b and 2c) in the case of a thin probe beam and strong photoelastic anisotropy ($|\xi_\pi| \gg 1$, $|\xi_d| \gtrsim 1$).

For large $|\xi_d|$, the shape of the curve for a long rod in the case of a wide probe beam differs significantly from the elastically isotropic approximation. This is due to the difference in the values of stresses σ_{zz}. The changes are concentrated near the [001] orientation (this is not the case in m3m crystals, see Section 3 in [5]), i.e., far from the [[A]] orientation, which is optimal under these conditions. The differences are less pronounced near the [011] orientation.

With strong birefringence and a thin probe beam, the stress σ_{zz} significantly affects depolarisation near the optimal orientation [[B]]. Changes are also most pronounced for large $|\xi_d|$, when [[B]] is close to [001]. Their mechanism is explained in Section 3 of [5] and in Section 4.2 of this work.

In media with negative ξ_π and missing critical orientation, the effect of elastic anisotropy on thermally induced depolarisation and the optimal orientations of the crystal axes are, on the whole, the same. However, the advantage of the [[A]] orientation in this case is more pronounced than for $\xi_\pi > 1$, since the value of $A_{2[[A]]}$ is much smaller {see (108) in [3]}. In particular, $A_{2[[A]]} = 0$ on the boundary of existence of the orientation [[C]] {(79) in [3]}. With weak birefringence, depolarisation is affected by the smallness of the effective thermo-optical constant Q^{eff}, and with strong birefringence, by the large effective value of the anisotropy parameter ξ^{eff} {see (108) in [3]}.

4.2. Case of $0 < \xi_\pi < 1$

At $|\xi_\pi| < 1$, the optimal degree of depolarisation in the elastically isotropic approximation for all orientations of the [*M*0*N*] type in the weak birefringence limit is constant as in m3m crystals, and in the absence of a critical orientation it is

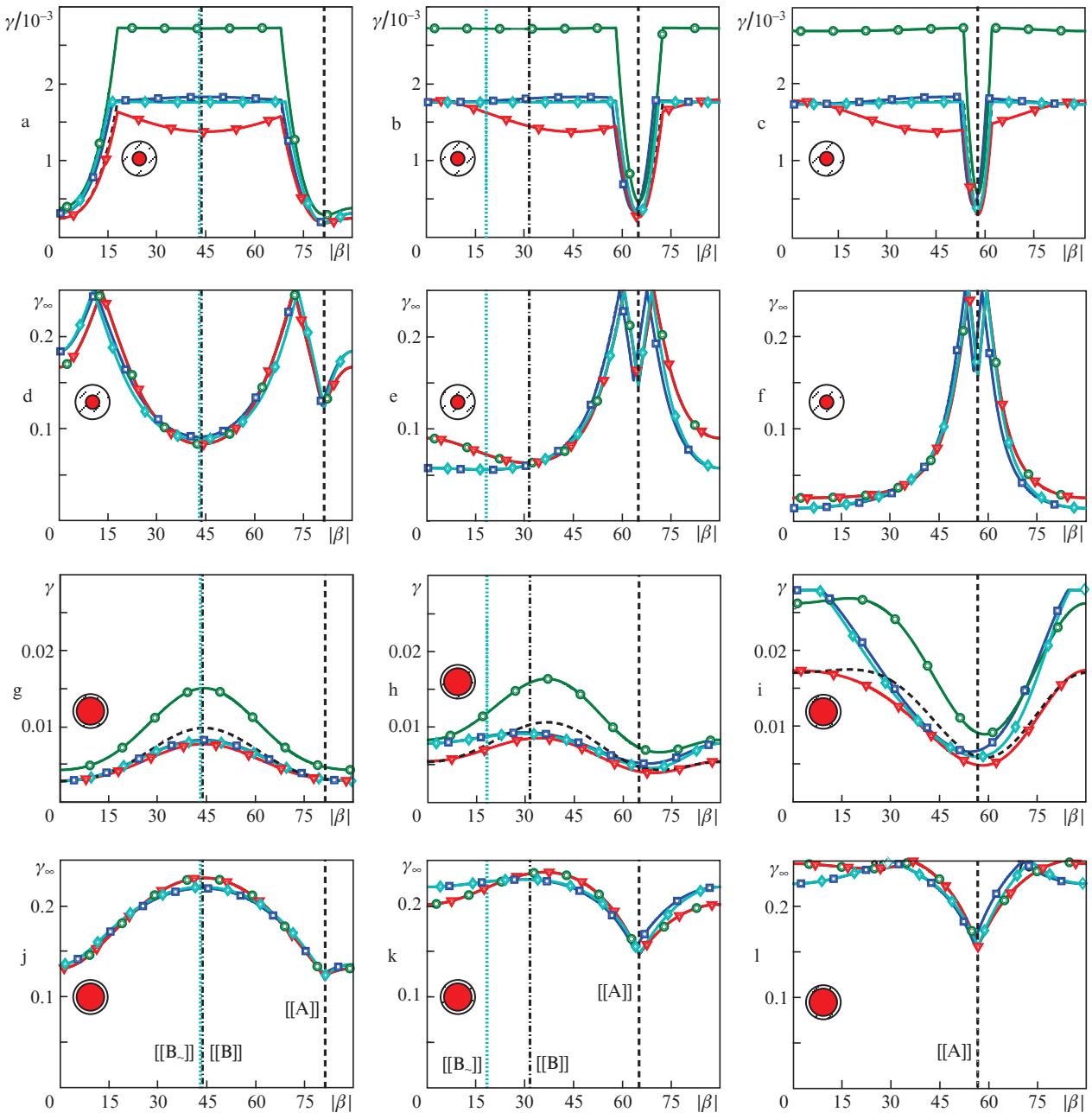

Figure 2. (Colour online) Calculated analytically optimal integral degrees of depolarisation for the orientations [*M*0*N*] ($\alpha = 0$) as functions of the Euler angle β in m3 crystals with elastic properties as in CaF_2, ξ_π as in YAG, ξ_d = (a, d, g, j) 0.1, (b, e, h, k) 1 and 2.3 (c, f, i, l) for $p = 1$ (a–c, g–i) and $p \gg 1$ (d–f, j–l). The calculations were performed in the elastically isotropic approximation (green circles, and for $p = 1$ also scaled black dashed curves), for a thin disk (red triangles) and for a long rod [the stress field was calculated by the complete (dark blue squares) and simplified (blue diamonds) Sirotin solutions]. The probe beam radius is $0.4R$ (a–f) and $0.8R$ (g–l), the beams are schematically shown in the form of circles. The specific orientations are marked with vertical lines and are shown in panels j–l.

also minimal among all orientations. Since, in addition, for [011] the degree of depolarisation does not depend on ξ_d [6], this property holds for all [*M*0*N*] orientations. In an elastically anisotropic crystal, the constancy of γ is violated by the dependence of elastic stresses on orientation, and the optimal orientation is entirely determined by the elastic properties of the medium.

Aleksandrov et al. [14] presented the measured values of the elastic stiffness tensor components and the following elasto-optic constants for Y_2O_3 and Sc_2O_3: $p_{11}-p_{21}$, p_{12}, and p_{66}. Unfortunately, this set does not make it possible to find either ξ_π or ξ_d. Moreover, the elasto-optic constants were found using a method that does not allow determining their sign.

However, if the second parameter of photoelastic anisotropy is assumed to be zero, the first can be estimated in absolute value, using the formula for an m3m crystal, and in both media it is less than unity (Table 1). In the weak birefringence approximation, the optimal degree of depolarisation for the [*M*0*N*] orientations is also independent of the sign of ξ_π, and so we assume for definiteness that $\xi_\pi > 0$ in sesquioxides. If this is not the case, then the error in our calculations will be

Table 1. Material parameters of sesquioxides [14].

Medium	ξ_π	ξ_d	ξ_s	$\nu_{[001]}$
Y_2O_3	$\pm 0.38(1 + \xi_d/2)$	N/A	0.65	0.38
Sc_2O_3	$\pm 0.64(1 + \xi_d/2)$	N/A	0.78	0.34

negligible, but the optimal orientation will be the critical one, for which the available data are insufficient to find the position.

Figure 3 shows the optimal integral degrees of depolarisation for the [$M0N$] orientations in two sesquioxides and in model crystals with $\xi_\pi = 0.2$ in the case of a wide probe beam with average birefringence. The curves are plotted for $\xi_d = 0$ and 0.5 (for clarity, in the case of sesquioxides, the curves are shown at a constant ξ_π corresponding to $\xi_d = 0$) (Table 1). The degrees of depolarisation at different ξ_d differ due to violation of the condition of smallness of birefringence, but very weakly. Optimal orientations at $\xi_d = 0.5$ deviate from the simplest ones also insignificantly. With this accuracy, the optimal orientations are determined in the same way as in m3m crystals (see Section 4.2 in [5]). In the elastically isotropic approximation, the degree of depolarisation is virtually constant. For a thin disk, the optimal orientation at $\xi_s > 1$ is [011], and at $\xi_s < 1$, [001]. In a long rod, the [001] orientation is almost always optimal. The variation in the degree of depolarisation for the [$M0N$] orientations is significant in the case of strong elastic anisotropy, when the simplified Sirotin solution is not accurate enough.

With strong birefringence, the [[A]] orientation, as for m3m crystals, ceases to be optimal starting from sufficiently wide probe beams, which is not observed at $\xi_\pi > 1$ (Fig. 4). An orientation close to [[B]] in the disk and to [[B$_\sim$]] in the rod becomes optimal; however, for wide probe beams, it significantly deviates from the specific orientation toward [001]. In disks, the degree of depolarisation coincides with the elastically isotropic one. In rods with large $|\xi_d|$, as the [[B$_\sim$]] orientation approaches [001], the magnitude of the stress σ_{zz} begins to exert a strong influence on the degree of depolarisation for optimal orientation. For $\xi_s > 1$ (Figs 4d–4f), the stress is

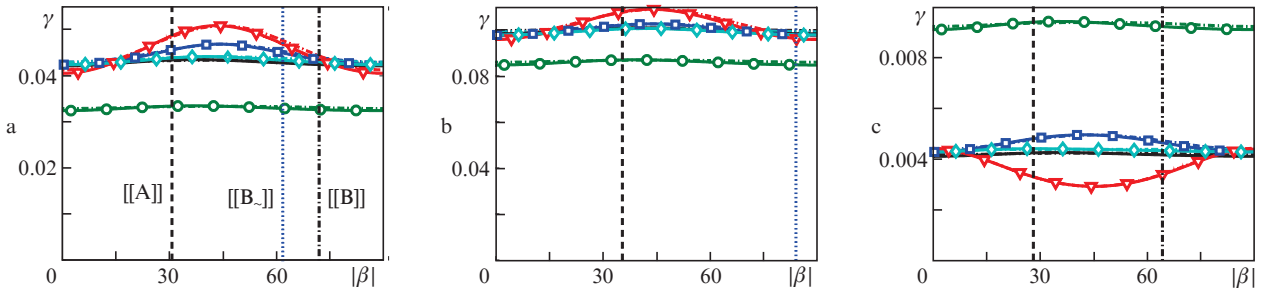

Figure 3. (Colour online) Calculated analytically optimal integral degrees of depolarisation for the orientations [$M0N$] ($\alpha = 0$) at $p = 10$ in disks (red triangles), long rods [the stress field is calculated by the complete (dark blue squares) and simplified (blue diamonds) Sirotin solutions] and in the elastically isotropic approximation (green circles and scaled plots, black curves) in (a) Y_2O_3, (b) Sc_2O_3 for $r_0 = 0.7R$ under the assumption of $\xi_d = 0$ (dash-dotted curves) and 0.5 (solid curves), as well as (c) in a medium with elastic properties as in KCl, $\xi_\pi = 0.2$ for the same r_0 and ξ_d. The specific orientations are marked for the case $\xi_d = 0.5$ and are shown in panel a.

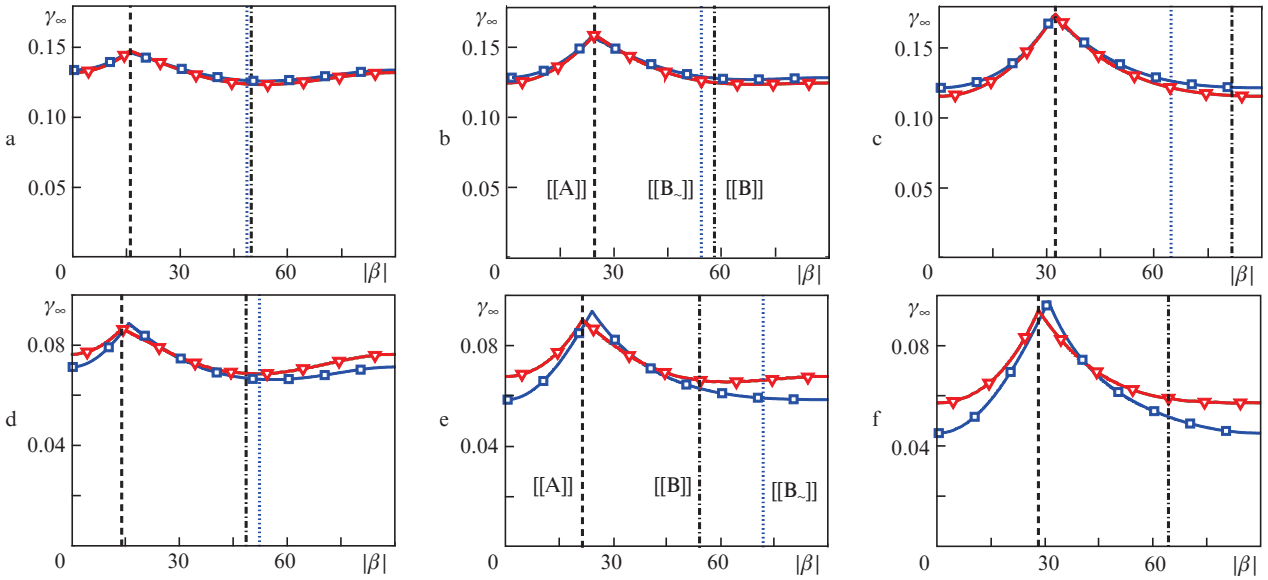

Figure 4. (Colour online) Calculated analytically optimal integral degrees of depolarisation for the orientations [$M0N$] ($\alpha = 0$) at $p \gg 1$ and $r_0 = 0.7R$ in the elastically isotropic approximation and a thin disk (red triangles), as well as in a long rod (blue squares) at $\xi_d =$ (a, d) 0.1, (b, e) 0.25, and (c, f) 0.5 in Y_2O_3 (a–c) and a medium with $\xi_\pi = 0.2$ and elastic properties as in KCl (d–f). The specific orientations are marked with vertical lines and are shown in panels b and e.

greater than the elastic isotropic one (see Fig. 3b in [5]); therefore, the effect of aligning the polarisations of eigenwaves in the central region of the active element, which weakens the depolarisation, is more pronounced than in the elastically isotropic approximation. For $\xi_s < 1$, the situation is the opposite (Figs 4a–4c). As noted in Section 4.1, this effect also occurs for $\xi_\pi > 1$.

Note that the degrees of depolarisation calculated for the stress fields obtained by the full and simplified Sirotin solutions are close. (Their greatest discrepancy is observed in the vicinity of the [[A]] orientation, i.e., far from the optimal one.) Therefore, in each Fig. 4, only one dependence is shown for a long rod.

5. Critical orientation for elastically anisotropic m3 single crystals

Like in m3m crystals, the critical orientation in m3 crystals in the case of a thin disk ([[C]]) is the same as in the elastically isotropic approximation {see formulae (80)–(82) in [3]}, and for a long rod [[Cs]] can deviate from this position (see Section 5.2.2 in [3]). Figure 5 shows the angles of deviation $\delta_{[[C]]}$ of the [[C_s]] orientation from the elastic isotropic estimate [[C]] for the rod, as well as the normalised integral depolarisation degree generalised to the case of m3 symmetry

$$\gamma'_N = \frac{\gamma([[C]])}{\min[\gamma([[A]]),([[B]]),\gamma([111])]} \tag{9}$$

for an orientation corresponding to this estimate, in media with $\nu_{[001]}$ and ξ_s as in CaF_2 (Figs 5a, 5b) and as in KCl (Fig. 5c) as functions of ξ_π at different ξ_d (Figs 5a, 5c) and of ξ_d at different ξ_π (Fig. 5b). One can see that the deviation of the critical orientation at moderate ξ_π, ξ_d, and ξ_s does not exceed several degrees. The loss in the degree of depolarisation under inaccurate tuning is significant only when both parameters of photoelastic anisotropy are large in magnitude simultaneously and is mainly due to the smallness of the degree of depolarisation for the [[A]] orientation due to its proximity to the critical orientation [[C_s]] [6] and, therefore, the smallness of the denominator in (9).

The decline of $\delta_{[[C]]}$ at $\xi_\pi < -3$ on the curves corresponding to $\xi_d = 3$ is due to the fact that the orientation [[C_s]] ceases to exist, merging with [[A_s]], which, as follows from the calculation algorithm, is optimal. At the same time, the orientation [[C]] for $\xi_s > 1$ continues to exist until it merges with [[A]]. In this case, $\gamma'_N \approx 1$. For $\xi_s < 1$, the orientation [[C_s]] deviates from [[C]] in the space of Euler angles to the other side, and [[C]] disappears for ξ_π smaller in modulus than [[C_s]].

6. Special cases of m3m and m3 crystals

It should be noted that there is a transition zone between the regions of parameters at which the dependence of the degree of depolarisation on orientation under weak birefringence is determined only by the elastic properties of the medium (see Section 4.2 of this work and Section 4.2 in [5]) and mainly by photoelastic properties (Section 4.1 of this work and Section 4.1 in [5]). With a relatively small excess of ξ_π over unity and a significant difference of ξ_s from it, both effects are significant. As follows from Fig. 3a from work [5], for $\xi_s > 1$, the elastic stresses in the disk with the [001] orientation are greater than those with the rest of the simplest orientations. An increase in the degree of depolarisation in the vicinity of the [001] orientation can lead to a change in the optimal orientation in m3m crystals and, at small values of $|\xi_d|$, in m3 crystals.

For simplicity, consider an m3m crystal. In the weak birefringence approximation, the degree of depolarisation in a thin disk is related to the elastically isotropic one as

$$\gamma = \gamma^{\text{iso}}/Z^2_{\text{disk}} \tag{10}$$

(see Section 5.1 in [3] and Section 4.1 in [5]). Therefore, the optimal integral degree of depolarisation for the [011] orientation will be less than for [001], provided the condition

$$R_\gamma(\xi_\pi) < R_z^2(\eta) \tag{11}$$

is met, where

$$R_\gamma(\xi_\pi) = \frac{\gamma^{\text{iso}}_{\text{opt}}([011])}{\gamma^{\text{iso}}_{\text{opt}}([001])}, \quad R_z(\eta) = \frac{Z_{\text{disk}}([011])}{Z_{\text{disk}}([001])},$$

$$\eta = (1 + \nu_{[001]})(\xi_s - 1),$$

in which the elastic and photoelastic parameters of the medium are separated. The quantity η was introduced in [3] with the opposite sign. Taking into account (32) and (39) from [3]

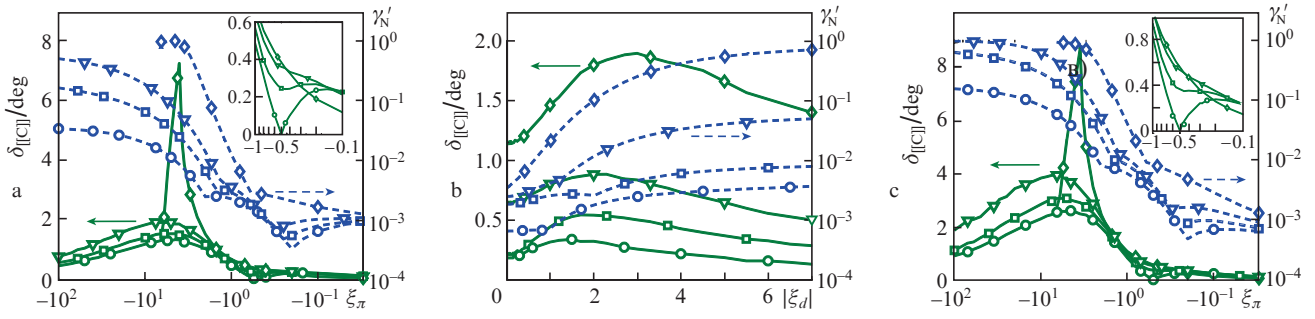

Figure 5. (Colour online) Angles $\delta_{[[C]]}$ of deviations of the direction [[C_s]] from the estimate [[C]] (solid curves), as well as normalised integral degrees of depolarisation for the orientation [[C]] γ'_N (dashed curves) in media with $\nu_{[001]}$ and ξ_s as in (a, b) CaF_2 and as in (c) KCl for $p = 3$ and $r_0 = 0.8R$: (a, c) dependences on ξ_π for $\xi_d = 0$ (circles), ± 0.6 (squares), ± 1 (triangles) and ± 3 (diamonds); (b) dependences on ξ_d at $\xi_\pi = -0.3$ (circles), -0.7 (squares), -1.2 (triangles) and -2.32 (diamonds).

$$R_z = \frac{1 + 7\eta/16}{1 + \eta/4}. \tag{12}$$

The R_γ value depends on the probe beam radius. For $r_0 = R$ and $r_0 \ll R$, respectively, we have

$$R_\gamma^{\text{big}}(\xi_\pi) = \frac{\min[\xi_\pi^2, G_{[011]}(\xi_\pi)]}{\min[\xi_\pi^2, 1]}, \qquad R_\gamma^{\text{small}}(\xi_\pi) = \max(\xi_\pi^2, 1), \tag{13}$$

where

$$G_{[011]} = \frac{(1 - \xi_\pi)^2}{8} + \frac{(3 + \xi_\pi)^2}{16}. \tag{14}$$

The values of R_z^2 and R_γ are shown in Fig. 6. At $\xi_\pi < 0$, the R_γ dependence is shown by dotted lines, since in the presence of a critical orientation, none of the compared orientations is optimal. Media with $\eta < -3/2$ do not exist {see (38) and (93) from [3]}.

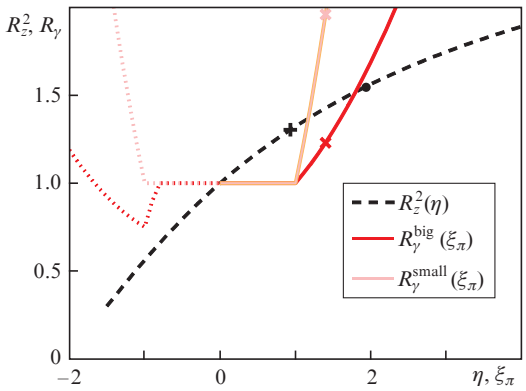

Figure 6. (Colour online) Quantities included in inequality (11). The values used to calculate the dependences in Fig. 7 are marked: $\xi_\pi = 1.4$ (×), $\eta(\text{KCl}) = 1.92$ (●) and $\eta(\text{CaF}_2) = 0.93$ (+).

Figure 7 shows the dependence of the degree of depolarisation on the Euler angle β for the orientations $[M0N]$ and $[MMN]$ in disks made of model m3m crystals with $\xi_\pi = 1.4$ and $\xi_s \sim 2$. For these media, $R_\gamma^{\text{big}} < R_z^2 < R_\gamma^{\text{small}}$ (see Fig. 6).

For comparison, we present the dependences in the elastically isotropic approximation, scaled for the purpose of approximate coincidence for the [001] orientation. While in the latter case, the optimal orientation is [001], in the elastically anisotropic solution for a wide probe beam (Figs 7b and 7c), the degree of depolarisation is minimal for the [011] orientation, and the [001] orientation may turn out to be the worst. With a decrease in the beam radius, the gain from using the [011] orientation decreases, and the orientation of the form $[MMN]$ becomes optimal, depending on ξ_π and elastic properties, in which the coefficient B_3/Z_{disk} entering into formula (72) from [3] is minimal, and the degree of depolarisation for the [001] orientation approaches this minimum (Fig. 7a). In general, in this range of parameters, the degree of depolarisation depends weakly on orientation, but qualitatively depends on the beam radius. Therefore, the optimal orientation is difficult to predict. With a decrease in the elastic anisotropy parameter, the considered effect weakens rapidly (Fig. 7c).

Comparing the orientations [001] and [011] for a long rod, one can obtain a relation similar to (11), but it will be more cumbersome, and the elastic and photoelastic properties of the medium in it will not be completely separated. As follows from Fig. 3a in [5], for a rod a value similar to R_z, as a rule, is less or slightly more than unity; therefore, the fulfilment of this inequality in real environments is unlikely. In numerical calculations for the parameters in question, the change in the optimal orientation also did not occur. Most likely, it will take place with a much more significant difference of ξ_s from unity. Analysis of Fig. 3a from [5] shows that at $\xi_s < 1$, the degree of depolarisation for the [111] orientation decreases, and therefore a dependence similar to that in Fig. 7a is possible. However, this would require a value of $\xi_s \sim 0.2$. We have not investigated this range of values as uncharacteristic for the crystals we know.

A similar behaviour of the degree of depolarisation is possible in m3 crystals. In a situation similar to Fig. 7a, the general orientation ($[MNP]$) will be optimal. With an increase in the probe beam radius, the optimal orientation will be close to [011] and shifted towards [[A]].

7. Conclusions

We have studied thermally induced depolarisation of a laser beam in cylindrical active elements in the form of a long rod and a thin disk made of single cubic syngony crystals of symmetry groups 23 and m3 with an anisotropic elastic stiffness tensor under volume uniform pumping and lateral heat

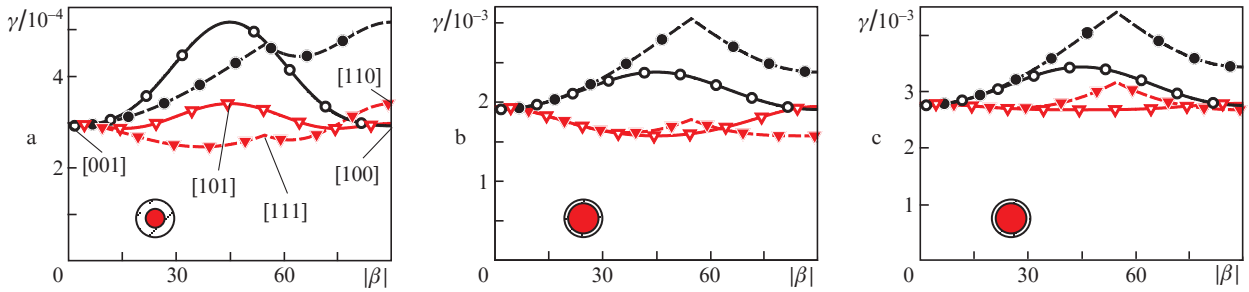

Figure 7. (Colour online) Calculated analytically optimal integral degrees of depolarisation as functions of the Euler angle β for the orientations $[M0N]$ ($\alpha = 0$, solid curves, empty symbols) and $[MMN]$ ($\alpha = \pi/4$, dashed curves, filled symbols) in model crystals with $\xi_\pi = 1.4$ and elastic properties as for (a, b) KCl and (c) CaF_2 at $p = 1$ for a thin disk (red triangles), as well as in the approximation of isotropic elasticity (black circles, dependences are scaled). The probe beam radii are (a) $0.5R$ and (b, c) $0.8R$; the simplest orientations are shown in panel a.

removal. The degree of thermally induced depolarisation is analysed as a function of orientation. The anisotropy of elastic properties affects this dependence. As for other cubic crystals, with weak birefringence the degree of depolarisation changes by a characteristic value of the order of tens of percent, and the shape of the dependence on orientation differs from the elastically isotropic one in different ways in the disk and the rod. The difference in the rod is most pronounced at a large value of the modulus of the second parameter of photoelastic anisotropy.

As in other cubic crystals, there are three ranges of values of the first parameter of photoelastic anisotropy ξ_π, in which elastic anisotropy affects differently the choice of the optimal orientation. For $|\xi_\pi| > 1$ and in the absence of a critical orientation, the optimal orientations in elastically anisotropic and elastically isotropic calculations, as a rule, differ by an amount of the order of several degrees. As in the elastically isotropic approximation, analytical estimates of the optimal orientations [[A]], [[B]], and [[$B_\sim$]] are accurate only for thin probe beams. Thus, for crystals of symmetry groups 23 and m3, the optimal orientations are shifted relative to both the specific orientations and the estimates in the isotropic elasticity approximation.

An exception to this rule for cubic crystals of any syngony is also considered. The emergence of a new optimal orientation, which is not specific, is demonstrated for strong anisotropy of the elastic stiffness tensor and weak anisotropy of the piezo-optical tensor.

For $0 < \xi_\pi < 1$ and with weak birefringence, the optimal orientation is determined by the elastic properties of the medium, practically does not depend on the photoelastic properties, and is close to either [001] or [011]. In the case of strong birefringence, the degree of depolarisation is optimal for the orientation [[B]] in the disk and for [[$B_\sim$]] in the rod in the case of a sufficiently large beam radius, which is not the case for $|\xi_\pi| > 1$. For a large value of the modulus of the second parameter of photoelastic anisotropy, the minimum degree of depolarisation differs significantly from the elastically isotropic one.

For $\xi_\pi < 0$, a critical orientation may exist for a crystal, for which thermally induced depolarisation vanishes in theory. The position of this orientation for the disk coincides with the elastically isotropic one, and for the rod it deviates from this direction. The angle of deviation, as a rule, is of the order of a degree, but it increases sharply at large values of both parameters of photoelastic anisotropy in absolute value.

Acknowledgements. The author considers it his pleasant duty to express his gratitude to E.A. Khazanov for the proposed topic and supervision of the work.

The work was supported by the World-Class Research Centre 'Photonics Centre' under the financial support of the Ministry of Science and High Education of the Russian Federation (Agreement No. 075-15-2020-906).

Appendix

Thermally induced beam distortions in laser ceramics made of elastically anisotropic cubic crystals

To date, we do not know any analytical solutions to the elasticity problem in elastic anisotropic laser ceramics. The problem is that in polycrystalline media, both the continuity of the strain tensor $\boldsymbol{u}$ (due to the continuity of the medium) and the continuity of the stress tensor $\boldsymbol{\sigma}$ (to satisfy the conditions of mechanical equilibrium) are required. However, the material elasticity equation (6) from [3] relating them contains a piecewise constant tensor coefficient $\boldsymbol{s}$ with discontinuities at the grain boundaries [16]. We assumed that the solution for ceramics is more complex and has variations in both strains and stresses within the crystallite. In the course of preliminary numerical simulation on an array of two-dimensional square granules with centres at the nodes of a square lattice, such a variation was demonstrated; however, it was relatively small for moderate values of the parameter $\xi_s \sim 2$. Preliminary calculations show that the presence of this variation increases small-scale thermally induced beam distortions in ceramics, but the addition to the spatial variation of the permittivity tensor [17] is also small. Moreover, since the scale of this additional variation is smaller than the grain size, its contribution to thermally induced beam distortions should be further weakened (see also [17]).

Unfortunately, the roughness of the used calculation model does not allow us to hope for the reliability of the quantitative results obtained. The construction of an analytical model in this case will also be significantly hampered by the statistical dependence of the variations of the elastic and photoelastic tensors, as well as by the nonlocality of the elasticity problem.

References

1. Koechner W. *Solid-state Laser Engineering* (Berlin: Springer-Verlag, 1999).
2. Mezenov A.V., Soms L.N., Stepanov A.I. *Termooptika tverdotel'nykh lazerov* (Thermo-Optics of Solid-State Lasers) (Leningrad: Mashinostroenie, 1986).
3. Vyatkin A.G., Khazanov E.A. *Quantum Electron.*, **50**, 114 (2020) [*Kvantovaya Elektron.*, **50**, 114 (2020)].
4. Sirotin Yu.I. *Kristallografiya*, **1**, 708 (1956).
5. Vyatkin A.G. *Quantum Electron.*, **51**, 565 (2021) [*Kvantovaya Elektron.*, **51**, 565 (2021)].
6. Vyatkin A.G., Khazanov E.A. *J. Opt. Soc. Am. B*, **28**, 805 (2011).
7. Mukhin I.B., Palashov O.V., Khazanov E.A., Ivanov I.A. *JETP Lett.*, **81**, 90 (2005) [*Pis'ma Zh. Eksp. Teor. Fiz.*, **81**, 120 (2005)].
8. Nye J.F. *Physical Properties of Crystals: Their Representation by Tensors and Matrices* (Oxford: Clarendon Press, 1957; Moscow: Inostrannaya literatura, 1960).
9. Khazanov E.A. *Opt. Lett.*, **27**, 716 (2002).
10. Turley J., Sines G. *J. Phys. D: Appl. Phys.*, **4**, 264 (1971).
11. Klopp P., Petrov V., Griebner U., et al. *Opt. Lett.*, **29**, 391 (2004).
12. Peters R., Kränkel C., et al. *Opt. Express*, **15**, 7075 (2007).
13. Baer C.R.E., Kränkel C., Saraceno C.J., Heckl O.H., Golling M., Peters R., Petermann K., et al. *Opt. Lett.*, **35**, 2302 (2010).
14. Aleksandrov V.I., Kitaeva V.F., Osiko V.V., Sobolev N.N., Tatarintsev V.M., Chistyi I.L. *Kr. Soobshch. Fiz. Fian*, (4), 8 (1976).
15. Nelson D.F., Vedam K., Cook Jr W.R. *High Frequency Properties of Dielectric Crystals – Piezooptic and Electrooptic Constants* (Berlin, Heidelberg: Springer-Verlag, 1996).
16. Hill R. *Proc. Phys. Soc. A*, **65**, 349 (1952).
17. Vyatkin A.G., Khazanov E.A. *J. Opt. Soc. Am. B*, **29**, 3307 (2012).